European Journal of Remote Sensing

ISSN: (Print) (Online) Journal homepage: www.tandfonline.com/journals/tejr20

Accuracy assessment of LAI, PAI and FCOVER from Sentinel-2 and GEDI for monitoring forests and their disturbance in Central Germany

Birgitta Putzenlechner, Felix Bevern, Philipp Koal, Simon Grieger, Martin Kappas, Tatjana Koukal, Markus Löw & Federico Filipponi

To cite this article: Birgitta Putzenlechner, Felix Bevern, Philipp Koal, Simon Grieger, Martin Kappas, Tatjana Koukal, Markus Löw & Federico Filipponi (2024) Accuracy assessment of LAI, PAI and FCOVER from Sentinel-2 and GEDI for monitoring forests and their disturbance in Central Germany, European Journal of Remote Sensing, 57:1, 2422323, DOI: 10.1080/22797254.2024.2422323

To link to this article: https://doi.org/10.1080/22797254.2024.2422323

Published online: 01 Nov 2024.

EUROPEAN JOURNAL OF REMOTE SENSING
2024, VOL. 57, NO. 1, 2422323
https://doi.org/10.1080/22797254.2024.2422323

Accuracy assessment of LAI, PAI and FCOVER from Sentinel-2 and GEDI for monitoring forests and their disturbance in Central Germany

Birgitta Putzenlechner[a], Felix Bevern[a], Philipp Koal[b], Simon Grieger[a], Martin Kappas[a], Tatjana Koukal[c], Markus Löw[c] and Federico Filipponi[d]

[a]Institute of Geography, Department of Cartography, GIS and Remote Sensing, Georg-August-University, Göttingen, Germany; [b]Forestry Research and Competence Centre, ThüringenForst AöR, Gotha, Germany; [c]Formerly Department of Forest Inventory, Federal Research and Training Centre for Forests Natural Hazards and Landscape (BFW), Wien, Austria; [d]Italian National Research Council – Institute of Environmental Geology and Geoengineering (CNR-IGAG), Montelibretti (RM), Italy

ABSTRACT

Forest monitoring benefits from biophysical parameters such as Leaf Area Index (LAI), Plant Area Index (PAI) and fractional vegetation cover (FCOVER) and can be obtained from optical and LiDAR remote sensing, such as Sentinel-2 (S2) and the Global Ecosystem Dynamics Investigation (GEDI). While GEDI-derived products consider all phyto-elements, those from S2 refer to green elements only. Apart from individual accuracies, systemic deviations among products are thus expectable. However, products from S2 and GEDI lack inter-comparison. We evaluated S2 and GEDI-derived LAI, PAI and FCOVER with digital hemispherical photography observations (DHP) in a forest disturbance hotspot in Germany across various forest conditions, including vital stands, standing deadwood and clearings. We found moderate to high agreement with in-situ data, with highest accuracy for S2-derived LAI ($R^2 = 0.54$) and GEDI-derived FCOVER ($R^2 = 0.73$). Agreements between S2 and GEDI products were low, which we attribute to systematic influences of woody components, GEDI's limitations in sloped terrain, and saturation of optical signals in dense canopy. In conclusion, findings suggest that while GEDI is effective in dense canopies, S2 products are beneficial for monitoring forest recovery. We also see potential for synergistic use in monitoring standing deadwood for habitat mapping and fire risk assessment.

ARTICLE HISTORY
Received 1 July 2024
Revised 19 September 2024
Accepted 11 October 2024

KEYWORDS
Biophysical variables; space-borne LiDAR; forest; disturbance

Introduction

Forests all over Central Europe are facing an increase of disturbance due to a variety of intensifying stressors (Patacca et al., 2023). Prolonged drought in the recent years has led to drought-related crown defoliation, early-season senescence, dieback as well as susceptibility to further stressors, such as insect and fungal infestations across different tree species (Senf et al., 2020). Given these rapid changes, satellite-based monitoring of forests is urgently needed as it provides spatially explicit information on the status of actual forest condition, understanding disturbance dynamics and extents as well as planning and monitoring forest restoration (Gao et al., 2020). Since its launch in 2015, data acquired within the Copernicus Sentinel-2 (S2) satellite mission at decametric spatial resolution is increasingly being used for operational forest monitoring (Phiri et al., 2020). In the meantime, space-borne LiDAR active sensors have emerged as well, such as the Global Ecosystem Dynamics Investigation (GEDI) (Schneider et al., 2020), with the potential to derive forest structure information with higher accuracy than from passive optical multi-spectral sensors.

Although forest changes are well-detectable from space, it remains challenging to translate the resulting products into quantitative information relevant for forest practitioners. Therefore, numerous algorithms have been developed for disturbance monitoring, which are mostly based on one or several different vegetation spectral indices to identify both abrupt and gradual changes (Löw & Koukal, 2020; Marinelli et al., 2023; Ochtyra et al., 2020). Although spectral indices deviations or retrieved disturbances are useful for anomaly detection, they do not represent biophysical variables that can be measured with physical units to allow for quantitative assessment of stand properties. In addition, such biophysical variables are crucial to link vegetation status to the C cycle (both fluxes and stocks) for global carbon balance assessments (Xiao et al., 2019). Leaf Area Index (LAI) and Plant Area Index (PAI) are defined as half of the total leaf and plant area per unit of the ground surface area, respectively, and represent crucial variables at the interface of biosphere and atmosphere, controlling forest productivity, interception, water and nutrient use as well as the carbon balance of (forest) ecosystems (Alton, 2016; Chen & Black, 1992; Ogutu et al., 2013;

CONTACT Birgitta Putzenlechner birgitta.putzenlechner@uni-goettingen.de Institute of Geography, Department of Cartography, GIS and Remote Sensing, Georg-August-University, Goldschmidtstr. 5, Göttingen 37077, Germany

Richardson et al., 2013; Sellers et al., 1997; Törnros & Menzel, 2014). For its key role for terrestrial ecosystems, LAI is one of the Essential Climate Variables stated by the Global Climate Observing System (GCOS) (2022). Another important biophysical variable is fractional vegetation cover (FCOVER), which is defined as the fraction of ground covered by vegetation (Liang & Wang, 2020). FCOVER is linked to forest health, disturbance dynamics and restoration as well as climate regulation and water cycling (Liang & Wang, 2020).

Although biophysical variables provide relevant information for decision-makers, existing remote-sensing-derived products are currently barely used in forestry practice. There are numerous products available from medium spatial resolution optical spaceborne sensors, such as MODIS, VIIRS or Proba-V (Lacaze et al., 2015; Yan et al., 2016, 2018), but limited by the fact that their spatial resolution is not detailed enough for forest applications. In this regard, biophysical products derived from S2 are promising and their retrieval is freely available with the Biophysical Processor implemented in ESA's free software "SNAP" (Weiss et al., 2020). There are implementations of different calibrated algorithms, that allow for retrieving biophysical variables both from the full set of spectral bands at 10 m and 20 m resolution (visible, red-edge, near-infrared and short-wave infrared spectral intervals) and the band set at 10 m resolution (visible and near-infrared spectral intervals). Due to their decametric resolution and a repetition rate of several days (under favourable sky conditions), the products are suitable for forest applications, but the different algorithms lack systematic inter-comparison and validation against reference data (Filipponi, 2021).

Although progress has been achieved to constantly improve algorithms to retrieve biophysical variables from optical remote sensing data, retrieval algorithms based on radiative transfer model inversion make simplifying assumptions on the canopy and rely on the unambiguity of spectral signatures for parameter retrieval (Richter et al., 2012a; Verrelst et al., 2015). For example, in their validation of the S2 biophysical products, Hu et al. (2020) found only moderate relationships (coefficients of determination 0.55–0.68) with the S2-derived LAI and FCOVER products against in-situ measurements in broadleaf forests. LAI is known to be less accurate for tall, dense or multi-layered canopy due to saturation of the spectral signal (Mutanga et al., 2023). As common algorithms typically focus on green vegetation elements (Djamai et al., 2019; Fernandes et al., 2014), there are limitations to detect woody and dry biomass that are dependent on species, phenology or vitality. Various attempts to retrieve structural information, e.g. from S2 data have ascertained the limitations of optical data (Kacic et al., 2023; Wernicke et al., 2022).

With the active sensing system, LiDAR provides more direct measurements of the canopy with higher potential to retrieve robust structural forest parameters (Brown et al., 2023). In particular, full waveform airborne LiDAR (ALS) has shown to yield robust estimates of forest structural variables, such as PAI and FCOVER in forests (Hu et al., 2018). Data availability of ALS is still limited and if existent, it is often not (freely) available. Although LiDAR satellite missions such as ICESat-2 have been used to retrieve LAI (Zhang et al., 2021), they have not explicitly focused on forest monitoring (Liu et al., 2021; Markus et al., 2017). In this regard, the GEDI instrument operated onboard the ISS, with its near infrared full waveform LiDAR, has been explicitly designed to retrieve structural vegetation parameters, thereby enabling new potentials for species and biodiversity mapping (Marselis et al., 2020; Schneider et al., 2020). While initial accuracy assessments have focused on canopy height (Adam et al., 2020; Liu et al., 2021; Potapov et al., 2021), the GEDI-derived PAI has been validated in several studies, showing promising performance across various forest biomes when validated against in-situ observations (e.g. digital hemispherical photography) and ALS (Brown et al., 2023; Wang et al., 2023a, 2023b). However, validation studies, both for GEDI and S2-derived biophysical variables, have focused on rather undisturbed, homogenous forests stands (Brown et al., 2020, 2023) so that product performances could be lower in actual forest disturbance settings. Specifically, in the context of actual forest disturbance, it is not clear how the GEDI products perform in disturbed forests with standing deadwood or on areas undergoing succession. Thus, as pointed out by Brown et al. (2023), validation against more in-situ measurements and different forest biomes is necessary to better understand actual performance.

Both the S2-derived and GEDI-derived products refer to effective LAI and PAI, i.e. assuming random distribution of leaves (Tang & Armston, 2019). Whereas the GEDI-derived products refer to all plant material, S2 products consider green vegetation elements only (Weiss et al., 2020). Thus, values of S2 products can be expected to be lower than GEDI products for a given canopy. However, we are not aware of an inter-comparison study of S2 and GEDI-derived LAI, PAI and FCOVER. Thus, there is the need to jointly assess (a) the accuracy of S2- and GEDI-derived biophysical variables in various forest settings, including factors affecting the level of agreement, and (b) if the products could be used complementary in forestry applications.

This study presents an accuracy assessment on S2- and GEDI-derived biophysical variables against in-situ observations from digital hemispherical photography (DHP) from two years (2021, 2022) in Central

Germany. We hypothesized that the level of agreement between S2- and GEDI-derived biophysical variables (i.e. LAI/PAI, FCOVER) varies depending on site-specific factors, i.e. terrain slope, amount of woody biomass, canopy height and forest type. Thus, our specific objectives were to (a) evaluate the consistency of S2-derived and GEDI-derived LAI/PAI and FCOVER, respectively, (b) evaluate the level of agreement between S2- and GEDI-derived products with regards to several impacting factors (i.e. canopy height, terrain slope, forest disturbance level) and (c) validate remote sensing derived products with in-situ observations. To obtain a realistic impression of the product performance and the comparability of optical products compared to LiDAR products, we deliberately examined stands so far understudied in validation studies, i.e. stands with standing deadwood, both open and very dense stands and cleared stands undergoing succession. We derive recommendations on the application potentials of S2 and GEDI products for practical forest monitoring in the context of forest disturbance.

Materials and methods

The methodological framework of this study is depicted in Figure 1, including the collection of in-situ (DHP and LAI-2200 measurements) as well as S2 and GEDI data and the performance evaluation, which was carried out as a product inter-comparison study and impact factor analysis of the agreement of S2 and GEDI products across the study area (see example in Figure 2b) as well as a validation exercise of S2 and GEDI products against in-situ observations at five study sites within the study area (Table 1).

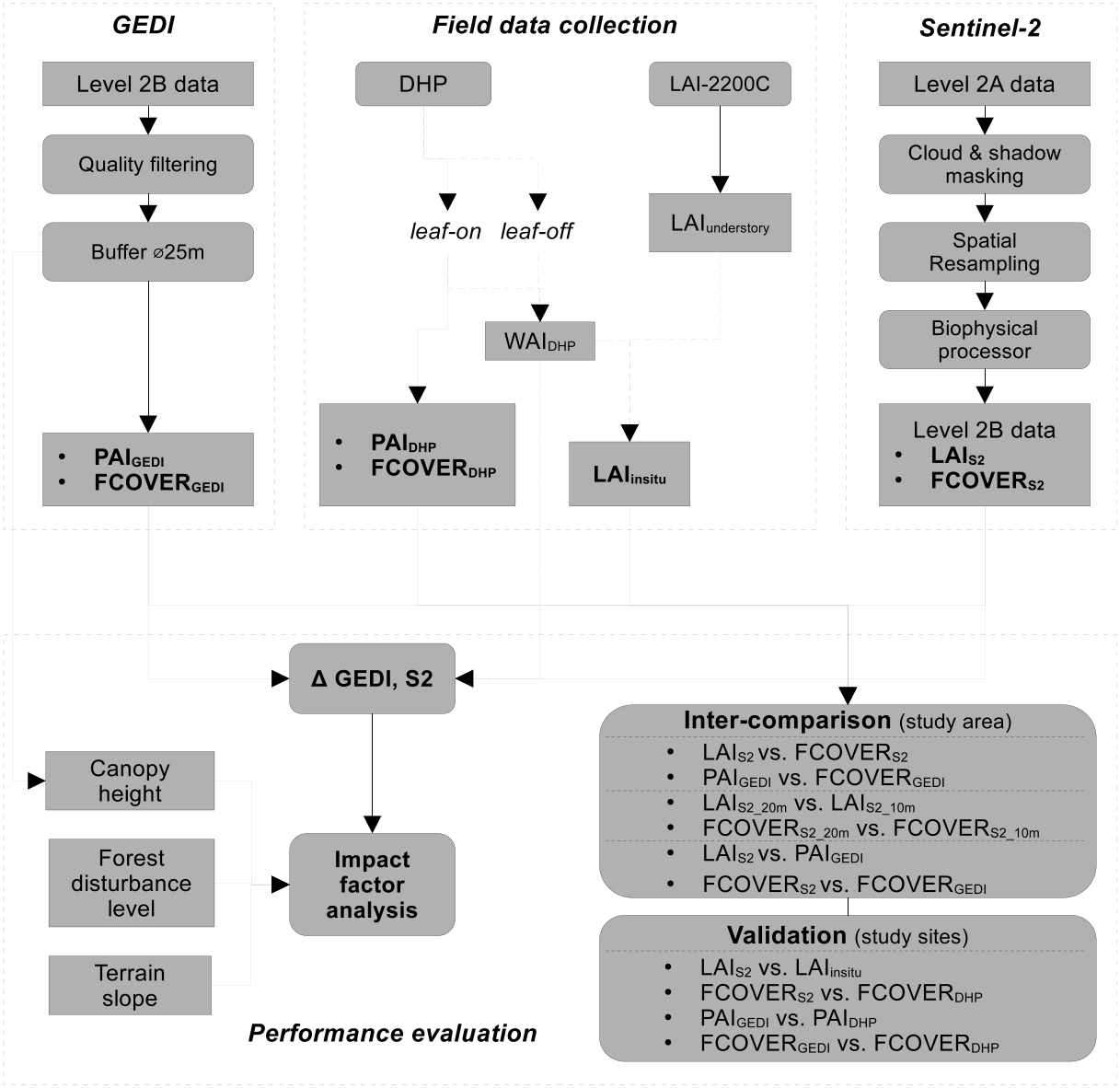

Figure 1. Methodological framework for retrieval, evaluation and validation of Sentinel-2- and GEDI-derived PAI, LAI and FCOVER products. Site-specific procedures to retrieve in-situ LAI for the validation of the S2-derived LAI product, considering contributions of WAI and understory vegetation, are illustrated with dashed lines.

Table 1. Characteristics of the study sites.

Site	Geographical location	Altitude (m a.s.l.)	Dominant tree species	Tree height (max in m)	Understory vegetation (dominant species)
Needleleaf, evergreen forest	51.616170 °N, 10.876900 °E	531	*Picea abies* (L.) Karst.	30	–
Broadleaf, deciduous forest I	51.608930 °N, 10.812816 °E	535	*Fagus sylvatica* L.	17	–
Broadleaf, deciduous forest II	51.612745 °N, 10.815332 °E	510	*Fagus sylvatica* L.	33	*Calamagrostis arundinacea*
Clear-cut	51.613921 °N, 10.806918 °E	502	-	-	*Senecio nemorensis, Calamagrostis arundinacea, Digitalis purpurea, Poa pratensis*
Standing deadwood	51.614576 °N, 10.808142 °E	506	*Picea abies* (L.) Karst.	23	*Rubus idaeus, Calamagrostis arundinacea, Urtica dioica*

Study area

The study area is located in Central Germany in the Southern Harz Mountains, a low mountain range, ranging from approx. 200 to 640 m.s.l. (Figure 2a,b). The area is characterized by all-year-round humid conditions, with mild summers and moderately cool winters. The mean annual temperature is 8°C, and mean annual precipitation sum is 760 mm (meteorological information taken from the "ReKIS platform" (Kronenberg et al., 2021)). Typical soil types are Cambisol, Podzol and Leptosol that formed on greywacke, rhyolite and sandstone as parent materials (ThüringenForst, 2022; TLUBN, 2006). Forests are composed of mostly even-aged Norway spruce (*Picea abies* (L.) Karst.) on the ridges (area share of 35% according to the local forest administration, "ThüringenForst") and deciduous stands of mostly European beech (*Fagus sylvatica* L.) at lower elevations and the southern facing slopes (area share of 53%). Recently, spruce stands have been affected by bark beetle infestation following several years of drought (2018–2020). To limit insect outbreaks, salvage logging has been practised. The resulting large areas of forest cover loss have been reported in remote sensing-based investigations, identifying the Harz as a hotspot of current forest cover loss in Germany (Kacic et al., 2023; Thonfeld et al., 2022).

Our study sites for in-situ data incorporate broadleaf and needleleaf forest stands of different age and density (Table 1). Within the sampling period between 2021 and 2023, these stands remained intact, so that comparability with GEDI data sampled one prior vegetation period at peak vegetation period or leaf-off season is ensured. Given the actual situation, we assessed post-disturbance plots, including standing deadwood and cleared areas undergoing succession and reforestation.

Remote sensing data

Pre-processing of Sentinel-2 Level 2B data

S2 satellite data acquired by the Multi-Spectral Instrument sensor in the period January 2021 – April 2023, with cloud cover lower than 90%, were gathered for the study area (granule T32UPC). Collected satellite acquisitions at processing level L2A are distributed by Copernicus as bottom of atmosphere reflectance, orthorectified, terrain-flattened and atmospherically corrected with the "Sen2Cor" algorithm (Richter et al., 2012b). S2 data were first processed to clip data to the study area, mask out invalid pixels (clouds, snow, shadows, topographic shadows), and spatially resample spectral bands and ancillary sun and view angle information at two common spatial resolution sets (10 m and 20 m). Images with less than 10% valid pixels resulting after masking were discarded. LAI and FCOVER biophysical variables were estimated using both the 10 m and 20 m bands within the SNAP "Biophysical Processor", version 2.0 (Djamai et al., 2019; Weiss et al., 2020). In order to compare the datasets generated using both versions of the implemented algorithm, estimates produced using the 20 m spectral bands were spatially resampled to 10 m spatial resolution, using the nearest neighbour resampling method. Dataset were finally spatially co-registered using AROSICS algorithm (Scheffler et al., 2017), in order to deal with weak spatial coherence of S2 time series processed using processing baselines 01.xx and 02.xx (Filipponi, 2019), improved under baselines 03.xx and 04.xx, and enhancing vegetation indices time series integrity (Filipponi et al., 2022).

GEDI Level 2B data

Data from NASA's GEDI mission was downloaded as "Level 2B Canopy Cover and Vertical Profile Metrics product" (GEDI02_B) from LP DAAC for the years 2019–2023. The biophysical metrics are derived from the Level 1B full waveform product based on the directional gap probability profile using the approach of Ni-Meister et al. (2001) (Dubayah et al., 2021b). The data is provided in HDF5 format at footprint level (25 m diameter). The R package "rGEDI" (Silva et al., 2020) was used to convert and subset the data to vector files.

GEDI delivers eight ground tracks with an across-distance of about 600 m and an along-track distance of about 60 m (Figure 2b). Each track contains (among other attributes) information on

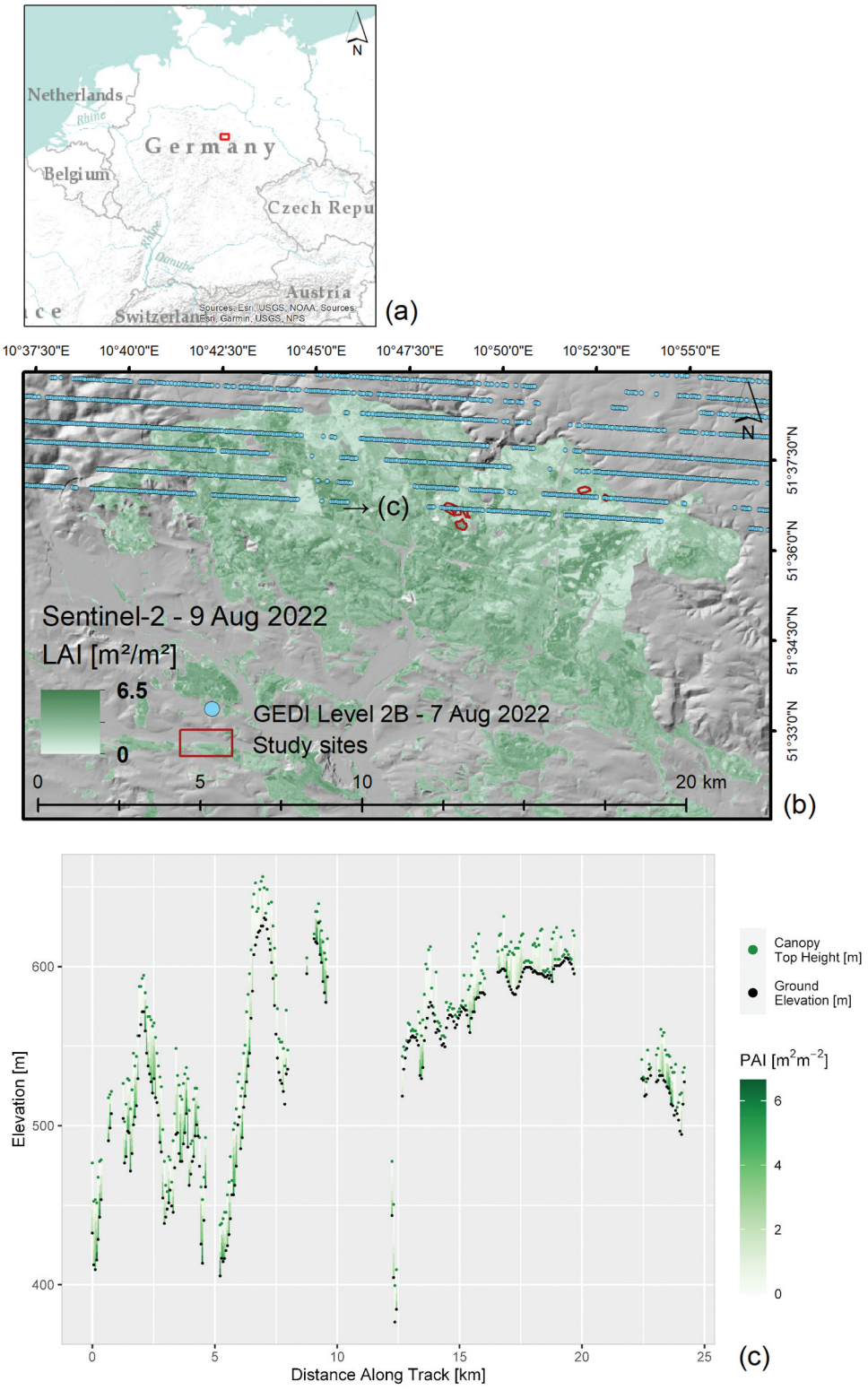

Figure 2. Location of the study area "Southern Harz Mountains" in Central Germany (a) and example of remote sensing products with Sentinel-2-derived LAI and GEDI level-2B product for close overpass dates in the summer of 2022 (b); selected GEDI track with PAI profile and terrain elevation across the study area (c).

canopy height and vertical profiles of biophysical variables calculated at 5 m bins (Figure 2c). For the inter-comparison with S2-derived biophysical variables and the validation against in-situ data, we focused on the attributes "pai" (total PAI), and "cover" (total cover) referred to as FCOVER in the following. We filtered the data using provided quality information (i.e. "L2B quality flag = 1", "L2A degrade flag = 0"), which may result in data gaps as depicted in Figure 2b,c. For information on canopy height shown in Figure 2c and used in an impact factor analysis, we used the attribute "rh100", i.e. maximum canopy height in centimetres from Level 2A data (Dubayah et al., 2021a).

Auxiliary geoinformation

Digital elevation model

We used a digital elevation model (DEM) at 5 m spatial resolution provided by the Free State of Thuringia (Landesamt für Bodenmanagement und Geoinformation, 2019). For consistency with S2 data, the DEM was formally transformed (i.e. EPSG: 25832 to EPSG: 32632) and resampled using cubic convolution before deriving terrain slope in degree.

Forest type classification

In the product inter-comparison and impact factor analysis, we distinguished between needleleaf and broadleaf forest stands, composed of Norway spruce and European beech as dominant species. Therefore, we used a classification map (provided by the forest administration) at 20 m spatial resolution based on S2 imagery, which was produced using a random forests classification approach in reference to Immitzer et al. (2019) and Persson et al. (2018) using administrative forest inventory data for training (Münder et al., 2022).

Forest disturbance information

It was our intention to quantify the level of agreement between S2 and GEDI products not only in healthy tall canopies but also in disturbed forest stands, including cleared areas undergoing succession (thus with presumably shorter canopies than the 5 m bins of the GEDI products) and standing deadwood. To retrieve information on forest disturbance, we used the outputs of an existing time series analysis framework by Löw and Koukal (2020). The approach utilizes dense S2 time series and a dynamic filtering for modelling phenology courses to detect phenological anomalies. Anomaly is calculated at pixel-level as the cumulative sum of daily differences between a baseline phenology course (calculated in a previous modelling period, here 2017–2018) and a smoothed time series at daily timestep for each pixel within a given detection period (here 2019–2021). Forest disturbance level (FDL) was calculated from the cumulative sum of daily deviations of the Normalized Difference Vegetation Index. The lower the FDL value, the longer the anomaly period and thus higher the severity of the disturbance. For details of the algorithm, the reader is referred to Löw and Koukal (2020).

Images of the study area (S2 granule "T32UPC") with a cloud cover of less than 80% were processed in the period between January 2017 and December 2021 (for details, see Putzenlechner et al. (2023)). Outputs of FDL, referring to (minimum) forest disturbance level by the end of 2021, were exported to GeoTIFF-format with 10 m spatial resolution and categorized. According to Löw and Koukal (2020), an FDL of −7 relates to unequivocal disturbance, such as standing deadwood or cleared areas. The FDL dataset was also used as a source of information to ensure that no disturbance occurred on the selected study sites in the vital beech and spruce stands.

In-situ LAI, PAI and FCOVER

Digital hemispherical photography

Digital hemispherical photography was used to retrieve effective PAI and FCOVER at the forested sites. The GEDI points with a footprint of 25 m were treated as Elementary Sampling Units (ESU). Locations were approached with a differential GNSS (model HiPer V, Topcon). To ensure sampling representativity and stable conditions, a total of 9–15 images were taken in the centre of the ESU as well as circularly-arranged within the footprint. Photos were taken upward with a full-frame digital camera (model Eos 6d mark ii, Canon) with 8 mm f/3.5 fish-eye lens (model Zenitar, Zenit) in diffuse or near-dusk conditions, using the "histogram method" to avoid overexposure recommended by Beckschäfer et al. (2013). The Can-Eye software was used (Weiss & Baret, 2017) to retrieve effective PAI (PAI_{DHP}) and FCOVER ($FCOVER_{DHP}$), considering zenith angles up to 60° and 10°, respectively. Camera calibration to determine the optical centre and projection function was carried out as described in the Can-Eye user manual (Weiss & Baret, 2017).

As GEDI data provision by LP DAAC took up to six months after acquisition, measurements had to be carried out at GEDI points from past overpasses. To quantify the contribution of woody canopy elements (WAI_{DHP}) in PAI, leaf-off DHP was carried out in the beech stands in April 2023. For spruce, WAI was retrieved in standing deadwood after needle-loss. Table 2 shows GEDI acquisitions and corresponding DHP acquisition dates for the study sites.

LAI measurements

On plots with herbal understory layer, i.e. within the standing deadwood and the open beech stand, LAI ($LAI_{understory}$) was acquired. Measurements were taken with the LAI-2200C (LAI-2200C Plant Canopy Analyzer, LI-COR Biosciences) at peak vegetation period (June to July) during clear-sky conditions around the solar noon to rule out shadowing of surrounding trees or trunks in the open spots. Per ESU (i.e. GEDI point), a total of 12 LAI samples were taken as recommended by Majasalmi et al. (2012) for open forests. The individual readings of the herbal layer were collected at non-tree-covered, un-shadowed spots, with below-canopy readings ("B-readings") preceded by above-canopy sequences for scattering correction ("K-records") required in direct sunlight conditions, following recommendations by LI-COR (LI-COR Biosciences, 2016). Mean effective LAI values of the

Table 2. Acquisition dates for DHP, GEDI and Sentinel-2 data and extracted samples obtained from overlapping GEDI tracks at the study sites. *No DHPs were taken on the cleared plot (PAI and FCOVER set as zero).

		GEDI			
DHP	S2	Beech (N = 12)	Spruce (N = 13)	Standing deadwood (N = 11)	Clearing* (N = 13)
30 Jul 2021	30 Jul 2021	23 Jun 2019		31 Jul 2020	11 Jul 2021*
14 Sep 2021	08 Sep 2021	23 Jun 2019	11 Jul 2021	11 Jul 2021	*
13 Oct 2021	01 Oct 2021		11 Jul 2021		*
01 Jun 2022	15 Jun 2022				*
06 Jul 2022	20 Jul 2022	02 May 2022	17 Sep 2021		*
29 Sep 2022	03 Sep 2022				*
06 Apr 2023	06 Apr 2023	26 Apr 2022			*

understory vegetation per study site accounted to up to 1.1 and 2.0 m^2 m^{-2} in standing deadwood and the open beech forest stand, respectively.

Considering contributions of understory and woody components for in-situ LAI

For validating S2-derived LAI, we assessed LAI_{insitu} considering contributions of WAI in PAI_{DHP} and the contribution of (green) understory vegetation. Depending on site characteristics (existence of deciduous canopy and/or understory herbal layer, Table 1), LAI_{insitu} was calculated following equations (1–3).

With PAI defined as the sum of LAI and WAI (Fang et al., 2019), the positive contribution of WAI to PAI has been accounted to 5 ± 35% (Bréda, 2003), with variations due to different species, phenological period, plant health status as well as contribution of the understory and combinations thereof. As PAI equals WAI in leaf-off conditions, LAI_{insitu} in the dense beech forest was assessed based on leaf-on and leaf-off DHP:

$$LAI_{insitu} = PAI_{DHP_{leaf-on}} - PAI_{DHP_{leaf-off}} \quad (1)$$

The contributions of WAI to PAI accounted to 20% in beech and 57% in spruce, respectively.

For LAI_{insitu} of standing deadwood, PAI_{DHP} and $LAI_{understory}$ were offset with each other depending on $FCOVER_{DHP}$:

$$LAI_{insitu} = PAI_{DHP} * FCOVER_{DHP} + LAI_{understory} * (1 - FCOVER_{DHP}) \quad (2)$$

For LAI_{insitu} of the open beech stand, equations (1) and (2) were combined:

$$LAI_{insitu} = \left(PAI_{DHP_{leaf-on}} - PAI_{DHP_{leaf-off}}\right) * FCOVER_{DHP} + LAI_{understory} * (1 - FCOVER_{DHP}) \quad (3)$$

Performance evaluation

Linking remote sensing with in-situ data

For product inter-comparison in the study area, GEDI acquisitions were matched to temporally nearest, cloud-free S2 acquisitions, resulting in 733 data points in either needleleaf or broadleaf forests for the years 2021 and 2022. GEDI data points (referring to single LiDAR shots) were buffered to account for the 25 m footprint and then intersected as ESUs with the S2 gridded products, which, in turn, were assigned to ESUs as spatially weighted averages.

For validation against in-situ data, GEDI tracks covering the five study sites were used to define initial locations for DHP acquisitions in 2021. The search was repeated to increase the number of samples and ensure even sampling numbers across the study sites. Overall, this procedure resulted in 49 samples available for comparison (Table 2). All spatial analysis was carried out in R with the "terra" package (Hijmans et al., 2023).

Product inter-comparison and validation

Product inter-comparison across the study area was carried out by investigating the relationships between LAI (PAI) and FCOVER products by fitting exponential and linear models between the two calibrated algorithm sets of the S2 products ("10 m bands version" vs. "20 m bands version") as well as between GEDI and S2 products. Observed WAI (at the study sites) was used to modify the "1:1 line" in the scatterplots for GEDI-derived PAI and S2-derived LAI.

For validation against in-situ observations, we performed linear regression and calculated several performance metrics, including the coefficient of determination (R^2) according to ordinary least square regression, the normalized root mean square error (nRMSE, using minimum-maximum-normalization), the mean bias error in percent (%bias) and the mean bias error (MBE). For evaluating performance of S2-derived LAI, we refer to the minimum required uncertainty of 20% for values ≥ 0.5 or 0.1 for smaller values set by the GCOS (2022). Further analysis focused on the "20 m version" of the S2 products, as the "20 m version" outperformed the "10 m version" (see results).

Impact factor analysis

The agreement between GEDI- and S2-derived products in broadleaf and needleleaf forests in the study area was investigated with linear and

generalized linear models (GLMs) and subsequent multi-factor analysis of variance (ANOVA) with post-hoc testing. While the deviation between the respective GEDI and S2 products (Δ GEDI, S2) was treated as target variable, covariables of the ANOVA were categories of canopy height, terrain slope and FDL. Due to the non-normal distribution of Δ PAI_{GEDI}, LAI_{S2}, a GLM with Gamma distribution was fitted, for which the value distribution of Δ PAI_{GEDI}, LAI_{S2} was shifted by the rounded absolute value of minimum Δ PAI_{GEDI}, LAI_{S2} to ensure positive value range required for the Gamma family. As overall measure of model fit, we calculated the R^2 and the Nagelkerke pseudo-R^2 (Nagelkerke, 1991) for the linear models and the GLMs, respectively.

Canopy height was aggregated into three categories to distinguish between juvenile (<15 m), established (15–35 m) and mature (>35 m) forest stands. Terrain slope was aggregated by means of the quantile method into four categories (<6°, 6° – 19°, 19° – 27°, > 27°). For FDL, we distinguished three categories, i.e. "undisturbed canopy" (FDL = 0), "somewhat disturbed canopy" (0 < FDL > −7) and "severely disturbed" (FDL ≤ −7) forests stands. Boxplots illustrate the results of post-hoc Tukey ($\alpha = 0.05$) testing with small letters. The WAI-related deviations between LAI and PAI (i.e. values of Δ PAI_{GEDI}, LAI_{S2} below observed WAI) are depicted as semi-transparent points.

Results

Inter-comparison of Sentinel-2 and GEDI products

PAI_{GEDI} and $FCOVER_{GEDI}$ as well as LAI_{S2} and $FCOVER_{S2}$ exhibit exponential relationships with high coefficient of determinations in both broadleaf and needleleaf forest stands (R^2 ~ 0.9, Figure 3). Thus, LAI_{S2} and PAI_{GEDI} saturate with increased vegetation cover. GEDI products are highly correlated due to their retrieval from directional gap probability (Dubayah et al., 2021b). In contrast, a higher spread of values exists between the S2 products in needleleaf forest stands ($R^2 = 0.86$).

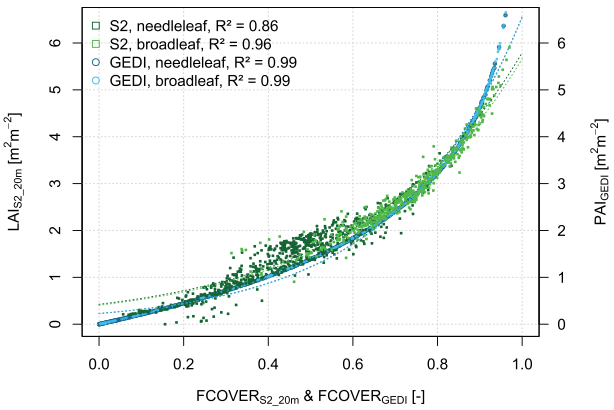

Figure 3. Sentinel-2 derived FCOVER against LAI as square symbols and GEDI-derived FCOVER against PAI in circles shown for needleleaf (dark green) and broadleaf (light green) forest in the study area. The dashed lines refer to fitted exponential models.

The different versions of the "Biophysical Processor" for the S2 products result in only minor differences between LAI and FCOVER products, respectively (R^2 > 0.8, Figure A1), with FCOVER products being more similar (R^2 ~ 0.9) irrespective of forest type. Considerable differences appear predominantly at higher LAI values (i.e. LAI > 4.0) and in broadleaf forest stands, thereby exceeding the GCOS uncertainty requirements (Figure A1a). This feature is also indicated for the different versions of FCOVER, but showing only marginal differences in needleleaf forest stands.

The inter-comparison of S2 and GEDI in the study area shows overall weak relationships (Figure 4), with higher coefficients of determination in needleleaf forest stands (R^2 ~ 0.2, Figure 4). However, bias is higher in needleleaf than in broadleaf forest stands (e.g. percent bias 11% vs. 6% for PAI/LAI). Considerable disagreement results from small values in GEDI products contrasting high values in S2 products. For example, it is noticeable that for high FCOVER values in the GEDI product (>0.8), there is still a considerable amount of low values of S2-derived FCOVER (Figure 4b).

Impact factor analysis

Linear (and generalized linear) regression models indicate effects of terrain slope and canopy height on deviations of GEDI and S2 products ($p < 0.05$), with R^2 for overall model evaluation ranging between 0.3 for ΔPAI_{GEDI}, LAI_{S2} and 0.4 for $\Delta FCOVER_{GEDI}$, $FCOVER_{S2}$, respectively. The effects of terrain slope and canopy height on ΔPAI_{GEDI}, LAI_{S2} are visualized in the boxplots in Figure 5 ($\Delta FCOVER_{GEDI}$, $FCOVER_{S2}$ in Figure A2). No distinct pattern was found for forest disturbance level, as indicated in value distributions of PAI and LAI (Figures 6 and A3).

Terrain slope. There are distinct differences between levels of slope for ΔPAI_{GEDI}, LAI_{S2} (and $\Delta FCOVER_{GEDI}$, $FCOVER_{S2}$), with decreasing agreement observed for stands on sloped terrain (Figures 5a and A2a). Here, values of the GEDI products tend to overpass those of S2 in broadleaf stands. For the LAI and PAI products, broadleaf stands on slopes above 19°, products show significantly less agreement, as absolute bias becomes highest.

Canopy height. There are also distinct differences for ΔPAI_{GEDI}, LAI_{S2} (and also $\Delta FCOVER_{GEDI}$, $FCOVER_{S2}$) between different levels of canopy height (Figures 5b and A2b). For low-growing canopy

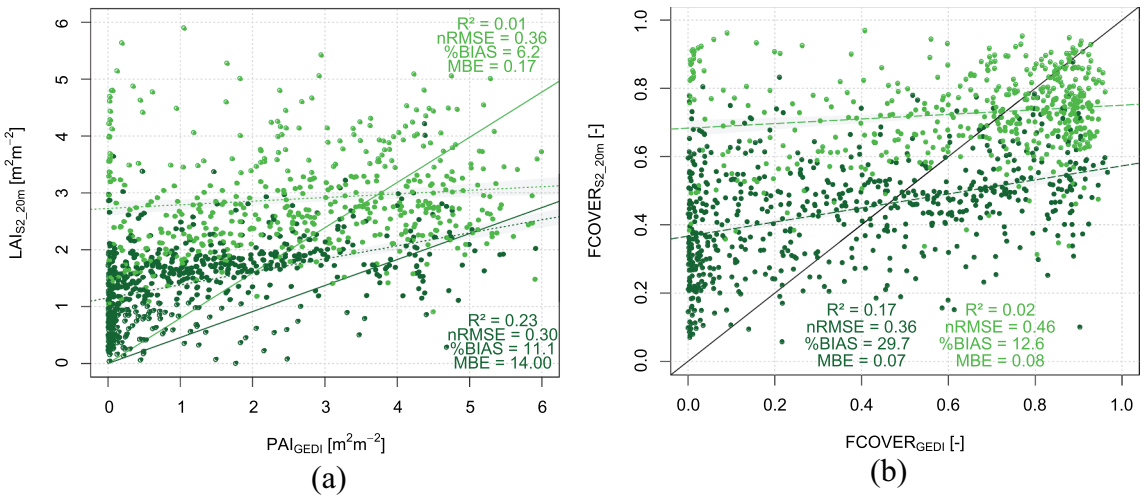

Figure 4. Sentinel-2-derived (a) LAI against GEDI-derived PAI and (b) FCOVER against GEDI-derived FCOVER in the study area 2021 and 2022. Needleleaf and broadleaf forests are coloured in dark and light green, respectively; for LAI/PAI (a), the continuous lines refer to the 1:1-line considering the observed PAI-to-LAI-bias. The grey-coloured polygons refer to the 90% confidence intervals for the linear regression models shown as dashed lines.

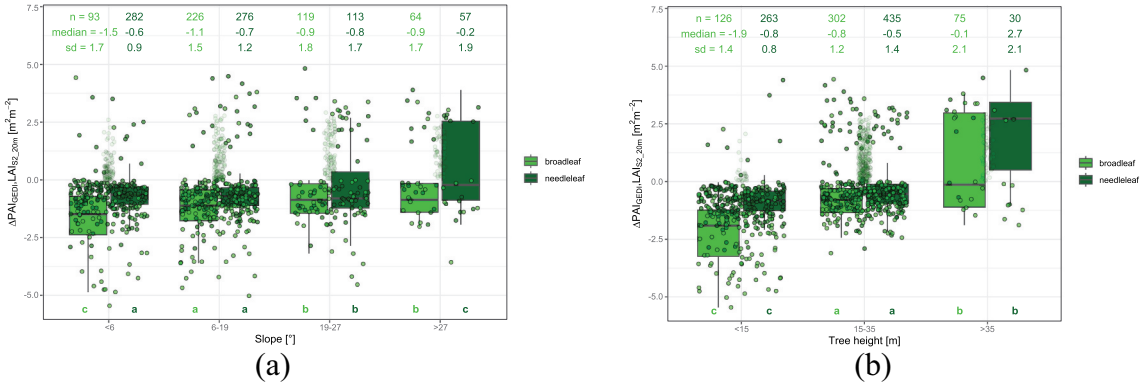

Figure 5. Deviation between GEDI-derived PAI and Sentinel-2-derived LAI with respect to (a) terrain slope and (b) canopy height for needleleaf and broadleaf forest in the study area in 2021 and 2022. Different lowercase letters indicate significant ($p < 0.05$) differences with levels of terrain slope for PAI deviations. Note that semi-transparent dots refer to deviations related to WAI.

(<15 m), the bias is negative (GEDI products < S2 products), whereas in tall canopies, values of GEDI products are higher than those of S2. This pattern is more pronounced in broadleaf stands but also observed for needleleaf stands. Overall, product agreement is best at canopy heights between 15 and 35 m as absolute bias is lowest.

Forest disturbance level. The GEDI and S2 products are consistent in showing considerably lower values of PAI, LAI and FCOVER on disturbed plots (Figures 6 and A3). Further, in needleleaf stands, values of all products are lower than in the corresponding disturbance level of broadleaf stands. However, in severely disturbed stands, GEDI values are close to zero, whereas the S2 products report PAI around 1.0 m^2 m^{-2} and FCOVER around 0.3 on average.

Validation against in-situ observations

Sentinel-2-derived LAI and FCOVER. S2-derived LAI and FCOVER were validated against in-situ measurements at GEDI locations. For S2, field measurements could be linked to S2 acquisition in a timely manner (Figure 7). The phenological dynamics are well-reflected in both the LAI and FCOVER products, with highest values in 2021 and 2022 reached by the end of June and an abrupt decline occurring after late September, indicating senescence (Figure 7). For LAI, highest values occurred in the dense beech forest and lowest values on bare areas and in standing deadwood, which is supported by in-situ LAI measurements and observations. For FCOVER, the dense beech stand also shows highest values, followed by vital spruce.

As for absolute values, the LAI and FCOVER values derived from S2 show overall considerable mismatch when compared to in-situ measurements (Figure 8). Linear regression models are significant but indicate low to moderate relationships (LAI: $R^2 = 0.5$), with best performance metrics for LAI_{S2} found for both versions of the algorithm (Figure 8a). However, for both LAI and FCOVER, the version of the algorithm including the 20 m bands performed slightly better compared to the version using the 10 m bands only. Overall, the S2 products underestimate in-situ measurements, with considerably

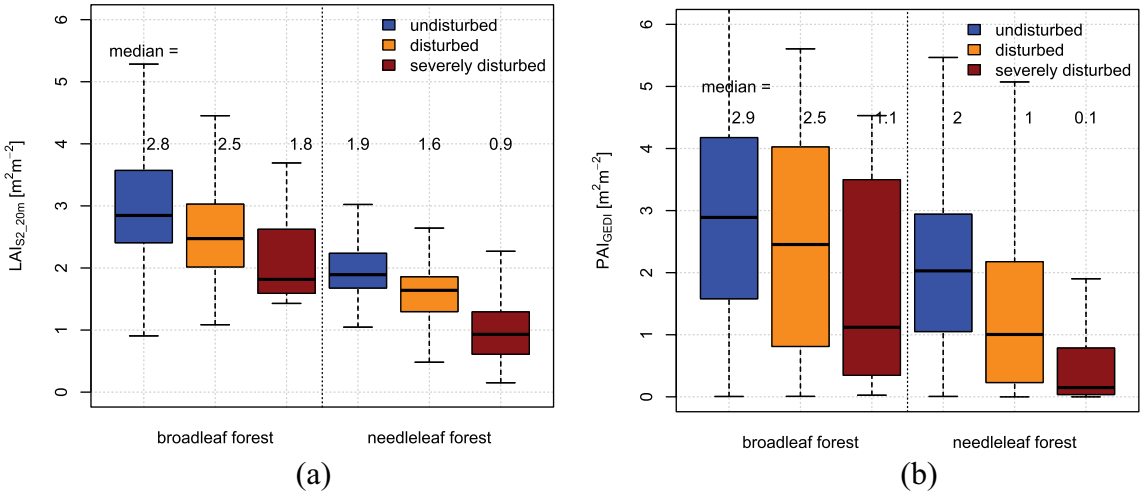

Figure 6. Sentinel-2-derived LAI (a) and GEDI-derived PAI (b) with regards to forest disturbance level and forest type.

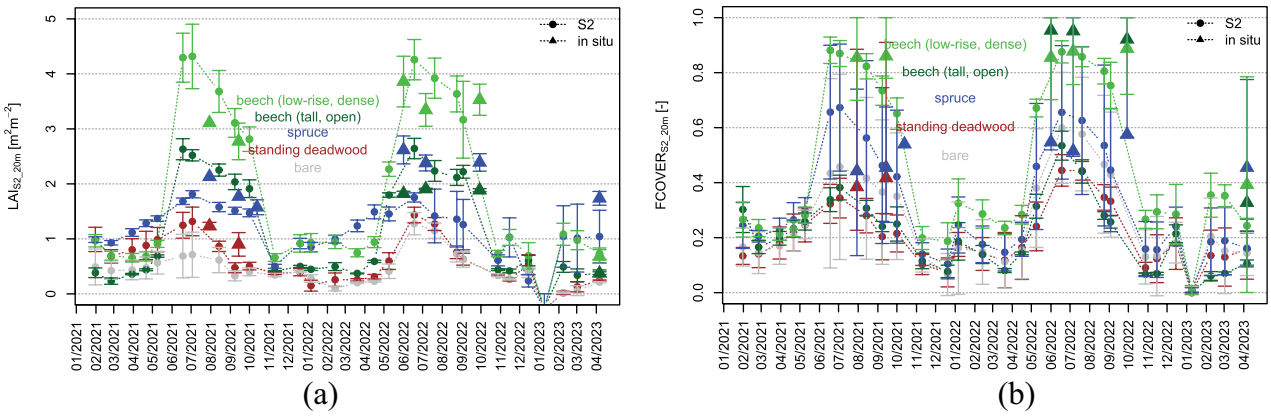

Figure 7. Time series of Sentinel-2-derived LAI (a) and FCOVER (b) and in-situ observations.

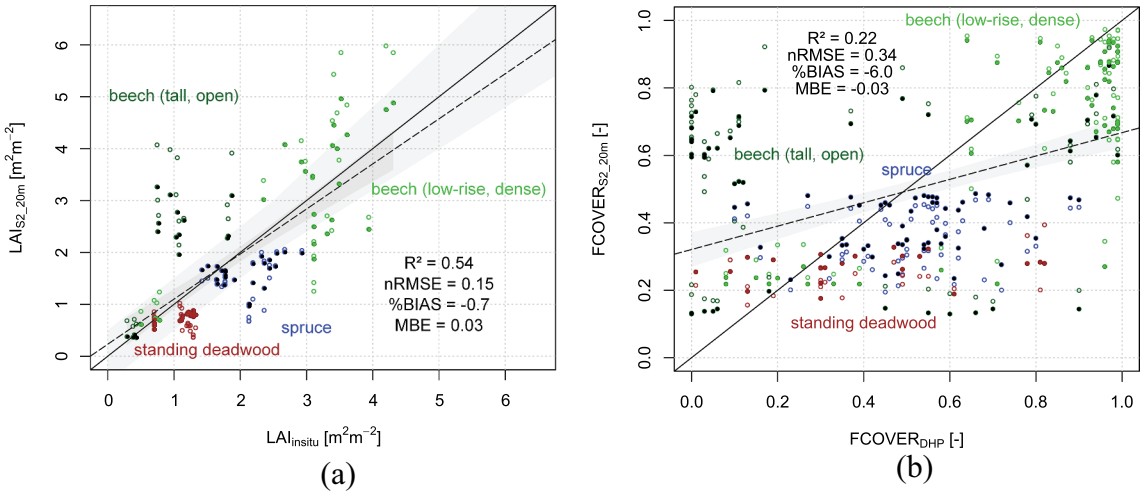

Figure 8. Sentinel-2-derived LAI (a) and FCOVER (b) against in-situ observations at the study sites. Both source band sets of the product retrieval algorithm are shown, with the version including also the 20 m bands shown with filled point symbols; performance metrics only refer to the 20 m version. The continuous lines correspond to the 1:1 line and the grey-coloured polygons refer to the 90% confidence intervals for the linear regression models shown as dashed lines. Note that for (a) LAI, the grey-coloured polygon around the 1:1 line refers to the GCOS uncertainty requirement.

higher bias observed for FCOVER compared to LAI (percent bias: −1% vs. 6%). Although LAI shows better performance than FCOVER, many observations fall outside the GCOS target uncertainty. The performance differs with study site: While in beech stands, LAI_{S2} tends to overestimate (especially in the tall, open stand), there is systematic underestimation in vital spruce and standing deadwood stands.

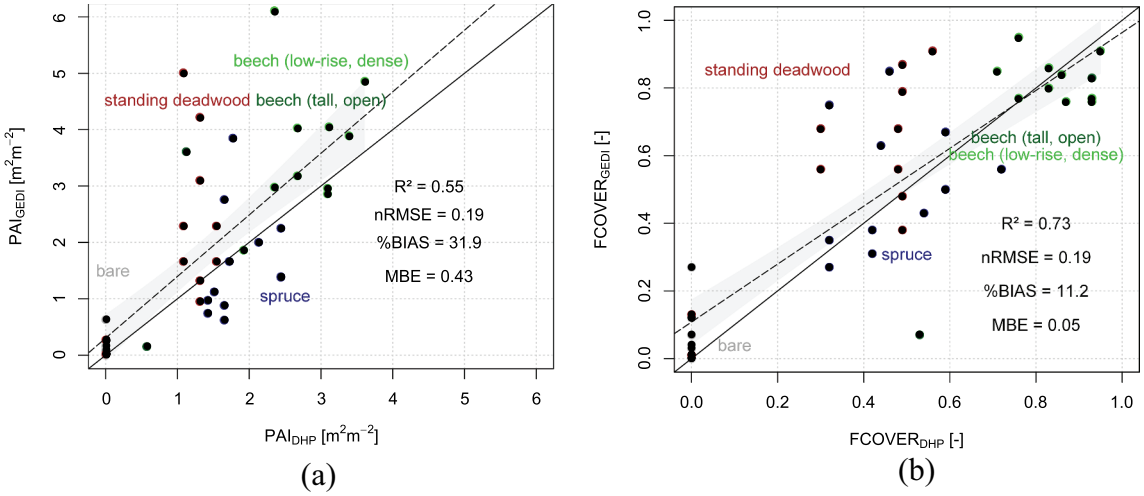

Figure 9. GEDI-derived PAI (a) and FCOVER (b) against in-situ observations at the study sites. The continuous lines correspond to the 1:1 line. The grey-coloured polygons refer to the 90% confidence intervals for the linear regression models shown as dashed lines.

GEDI-derived PAI and FCOVER. Compared to the results from S2 product validation, GEDI products perform better when validated against in-situ measurements from DHP (Figure 9). Best agreement is obtained for FCOVER, showing a significant linear regression model with relatively high coefficient of determination (R^2 ~ 0.7). Overall, GEDI products tend to overestimate in-situ observations, with percent bias between 11% and 32% for FCOVER and PAI, respectively. As for S2, GEDI's product performance is site-dependent, with high accuracy in the beech stands and relatively low agreement in spruce, especially standing deadwood. Clear-cut areas show low PAI values below 1 and FCOVER below 0.3, which may indicate a certain sensitivity to remaining lying deadwood.

Discussion

Evaluation of the experimental design

In this study, we used DHP for retrieving effective PAI and FCOVER. Thus, our approach incorporates a general disparity between downward-looking remote sensing systems and upward-looking DHP. Nevertheless, we have designed the approach in the best possible way to eliminate uncertainties in the accuracy assessment. We performed leaf-off measurements to derive WAI and thereby accounted for the difference between PAI and LAI that were often treated as interchangeable quantities (Chen et al., 2023). We incorporated an understory correction for LAI, since it is known that understory reflectance can significantly influence forest reflection (Rautiainen et al., 2018). Since evaluation between the remote sensing products exhibited higher deviation than evaluating remote sensing products against the in-situ measurements, we deem our reference measurements valid.

We deliberately included sites that were considered challenging, e.g. by including dense or clumped canopy and disturbed sites with standing deadwood, and this could explain the overall low to moderate relationships we observed for S2 and GEDI products with in-situ observations. It should be noted that sampling numbers were relatively low which is because we oriented our sampling design in line with the GEDI observations to facilitate the most direct comparison, akin to the methodology employed by Wang (2023b). Apart from the fact that our study area is at the edges of the GEDI coverage of the northern hemisphere, high-quality data was rare as well. It was due to the scarcity of GEDI data that the temporal consistency of GEDI-derived PAI and FCOVER could not be investigated. In addition, the availability of GEDI data leads to time lags between GEDI observations and actual in-situ data collection. Nevertheless, we were able to counteract this by using the disturbance area product to rule out observed deviations between datasets due to intermediate disturbance in the respective pixels.

Accuracy of Sentinel-2 and GEDI products

Between LAI/PAI and FCOVER, we obtained a high agreement from an exponential fit (Figure 3), which is in agreement with field and simulations studies (Eriksson & Eklundh, 2005; Mougin et al., 2014). The lower coefficient of determination for the S2 products could arise from higher variability in the optical data, i.e. variations in leaf pigments, phenological changes of the understory vegetation, as well as directional and atmospheric fluctuations affecting the accuracy of LAI retrievals (Fang et al., 2019). In particular, the lower accuracy observed at the beech stands

(compared to spruce) could result from seasonal variations of chlorophyll.

S2-derived LAI and FCOVER were consistent with in-situ observations concerning seasonal variations and value proportions at the study sites (Figure 7). The overall low (FCOVER) to moderate (LAI) linear relationships (Figure 8) obtained in validation against in-situ observations widely agrees with existing studies (also based on DHP and S2 products), reporting coefficients of determination for LAI between 0.33 (Chen et al., 2023) and 0.68 (Hu et al., 2020) and for FCOVER of 0.55 (Hu et al., 2020). The overall higher accuracy of LAI compared to FCOVER as well as the overestimation bias for LAI is in accordance with Hu et al. (2020) (bias: 0.42). While the underestimation bias of LAI in spruce and standing deadwood could be related to uncertainties of DHP retrieval for clumped canopy (Lee et al., 2023), the retrieval in the dense beech stand could be affected by saturation effects occurring with high LAI values (Fang et al., 2019). As variations in the NIR and SWIR are known to describe effective LAI best (Heiskanen et al., 2013), saturation effects could be more pronounced with less spectral information, which could explain better performance of the LAI product considering also the 20 m bands (Figure 8a). Indeed, in their sensitivity analysis for deriving GEDI attributes from S2 data, Kacic et al. (2023) found the Red Edge bands to be most decisive. Thus, the additional information contained in the Red Edge could compensate the disadvantage of lower spatial resolution of the 20 m bands compared to the 10 m bands. The low effect of different product versions for the performance of S2-derived FCOVER (Figure 8b) could result from the fact that both products showed low accuracy, which may indicate the general difficulty in deriving this variable from optical data.

Compared to the S2 products, accuracy of GEDI-derived PAI and FCOVER was higher (Figure 9), which can be attributed to the better suitability of LiDAR to retrieve forest structure variables. Our results for PAI (RMSE = 1.16, nRMSE = 0.19, Figure 9a) widely agree with existing studies (Brown et al., 2023; Chen et al., 2023; Wang et al., 2023a), reporting RMSE between 0.7 and 1.0. Accuracy was decreased in standing deadwood compared to vital stands, which is in accordance with findings of Wang et al. (2023b) who reported lower accuracy for leaf-off observations. The overall similar performance observed at the needleleaf and broadleaf stands differs from findings of C. Wang et al. (2023a) who report better agreement in needleleaf canopies. Overall, there is still a limited sampling number among validation studies for GEDI-derived PAI, even though moderate to high relationships with in-situ observations were reported. Regarding FCOVER, our results indicate high capabilities of the GEDI product. However, more studies are needed for performance evaluation, as validation studies on canopy attributes have so far mainly focused on canopy height and PAI (Adam et al., 2020; Brown et al., 2023; Chen et al., 2023; Dorado-Roda et al., 2021; Wang et al., 2023a, 2023b). Nevertheless, the better performance of GEDI-derived FCOVER in the dense beech stand (Figure 9b) could support findings of Dorado-Roda et al. (2021), who reported better performance in dense canopy.

Consistency of S2 and GEDI products and potentials for forest monitoring

The inter-comparison of S2 and GEDI products revealed weak relationships (highest $R^2 \sim 0.2$ obtained for LAI vs. PAI in beech, Figure 7a). The positive bias between GEDI-derived PAI and S2-derived LAI can be attributed to the conceptual differences of the quantities, i.e. contributions of WAI, which is also in line with the higher bias found in needleleaf stands. Here, our results are in accordance with Chen et al. (2023), reporting coefficients of determination between 0.23 and 0.35 for PAI vs. LAI. Based on our results, the low agreements result from product mismatches in the lower, but for the most part upper value ranges. The mismatch in the higher value ranges may be attributed to (previously discussed) saturation effects of the S2 products and in the lower value ranges to potential geolocation inaccuracies (10.2 m in Level2B version 2, Dubayah & Blair, 2021a). After all, we attribute the mismatch to the conceptual differences between passive optical and LiDAR data. For example, Wernicke et al. (2022) reported low explanatory potential of S2 data for forest structure compared to aerial LiDAR data, thereby also classifying results from Kacic et al. (2023), who faced challenges in modelling GEDI biophysical attributes from S2 data (among other) with random forest regression.

The effect of terrain slope on the deviations between GEDI and S2 products (Figure 5a) is in accordance with findings of numerous studies reporting uncertainties of GEDI attributes in steep terrain (Adam et al., 2020; Chen et al., 2023; Fayad et al., 2021; Schneider et al., 2020), even if estimates vary as to the threshold at which errors become critical (e.g. >20° in Adam et al., 2020; > 30° in Liu et al., 2021). With significant effects observed at slopes above 19°, we recommend filtering out such data, as carried out in recent studies with varying thresholds (Chen et al., 2023; Stritih et al., 2023). Regarding canopy height, we found significantly increased deviations between products in very high and low canopies (Figure 5b). Although their analysis was on the accuracy of canopy height, Liu et al. (2021) reported higher errors of GEDI estimates in tall dense canopies which in turn, Brown et al. (2023) did not confirm in their validation study on PAI. In tall stands, deviations may, however,

also increase due to the uncertainty of S2 estimates associated with the saturation of the optical signal, as mentioned previously. We found no distinct pattern in product deviations across different levels of forest disturbance. Consistently low PAI/LAI and FCOVER in disturbed needleleaf forest stands can be attributed to salvage logging which has been carried out in the study area due to bark beetle infestation of Norway spruce. Based on the observations on the cleared study site, the first bin of GEDI (i.e. <5 m) seemed sensitive to remaining lying deadwood (Figure 6), while the considerably higher values of the S2 products can be attributed to green (herbal) vegetation which are not detectable with GEDI.

To summarize our findings with regards to product potentials for monitoring forest and recovery, we found that S2-derived LAI and FCOVER are appropriate for monitoring initial succession, if woody components are out of interest. Given our findings that LAI and FCOVER reached similar value ranges in vital forest stands, we consider GEDI products better suited for overall forest delineation. In addition, these products demonstrated high potential to also characterize standing deadwood. Thus, synergic use of S2 and GEDI products could be exploited to detect deadwood structures and monitor succession which is relevant for recovery management, biodiversity or fire risk assessment.

Conclusion

We evaluated the performance and comparability of LAI, PAI and FCOVER derived from Sentinel-2 (S2) and GEDI for forest monitoring between 2021 and 2023 in Central Germany. In the context of recent forest disturbance across Central Europe, we deliberately investigated study sites considered challenging for both LiDAR and optical sensors, i.e. stands with dense and open stands with understory, cleared sites undergoing succession and standing deadwood. As such, the study aimed at a realistic assessment of the performance of S2- and GEDI-derived canopy attributes with regards to forest monitoring. Therefore, we also assessed the deviations between S2- and GEDI-derived products with regards to influencing factors, i.e. terrain slope, canopy height and forest disturbance level.

Both the S2 and GEDI products were consistent within each other, and phenological variations were well-reflected in S2-derived LAI and FCOVER. Further, both S2 and GEDI products showed consistently lower LAI, PAI and FCOVER on disturbed sites and peaked in dense stands with broadleaf canopy. While GEDI-derived FCOVER showed best performance ($R^2 \sim 0.7$) when validated with in-situ observations, LAI and PAI products reached moderate performance ($0.5 > R^2 < 0.6$). For S2 products, we attribute limitations mainly to saturation effects and the generic nature of the algorithm. Although GEDI's performance was higher, we encountered limitations due to data availability and timeliness, thereby stressing the need for a future LiDAR satellite mission. The inter-comparison of GEDI and S2 products revealed low overall agreement, which was significantly aggravated on stands with sloped terrain and in tallest stands. Overall, the deviations can be attributed to conceptual differences, with the S2 and GEDI products focusing on either green or woody vegetation components, respectively.

Our findings emphasize different application potentials of the products, and we therefore recommend that products should be used rather complementarily (instead of interchangeably). While monitoring stand properties or the delineation of forests with S2-derived LAI and FCOVER alone would be difficult, products are beneficial for monitoring temporal dynamics of forest rejuvenation and succession. GEDI-derived PAI and FCOVER hold great potential for stand characterization and forest delineation. Further, in the context of forest recovery, these attributes could be used for implications on microclimate. For future studies, we see synergetic potential for a differential recovery monitoring, including deadwood structures, rejuvenation and succession. An integrated approach could be based on detecting forest disturbance from S2 time series, identification of structural components with space-borne LiDAR on disturbed plots and monitoring vegetation recovery with the S2 biophysical products. Ultimately, the complementary or even synergistic use of optical and LiDAR remote sensing will be crucial for comprehensive forest monitoring, including biodiversity and fire risk assessments in post-disturbance landscapes.

Acknowledgments

The authors thank the Federal Research and Training Centre for Forests Natural Hazards and Landscape (BFW), Austria, for providing resources to apply the forest disturbance modelling framework. The authors acknowledge the support of Lajos Blume with maintenance as well as Ingolf Profft (FFK Gotha, ThüringenForst), Gerhard Thomsen, Stefan Großer (both forest administration Bleicherode-Südharz) and Erik Speitling (Klosterkammer Hannover) for the ongoing collaboration at the study sites. This work contains modified Copernicus Sentinel data (2024).

Disclosure statement

No potential conflict of interest was reported by the author(s).

Funding

This work was supported by the Federal Ministry of Education and Research (BMBF) under Grant 033L304B.

Author contributions

BP: Conceptualization, methodology, formal analysis, data curation, investigation, writing – original draft, visualization; FB: Data curation, formal analysis, writing – review and editing; PK: Data curation, methodology, writing – review and editing; SG: Methodology, writing – review and editing; MK: Resources, writing – review and editing; TK: Resources, writing – review and editing; ML: Software, writing – review and editing; FF: Conceptualization, software, writing – review and editing.

Data availability statement

The data that support the findings of this study are available from the corresponding author, BP, upon reasonable request.

References

Adam, M., Urbazaev, M., Dubois, C., & Schmullius, C. (2020). Accuracy assessment of GEDI terrain elevation and canopy height estimates in European temperate forests: Influence of environmental and acquisition parameters. *Remote Sensing*, *12*(23), 3948. https://doi.org/10.3390/rs12233948

Alton, P. B. (2016). The sensitivity of models of gross primary productivity to meteorological and leaf area forcing: A comparison between a Penman–Monteith ecophysiological approach and the MODIS light-use efficiency algorithm. *Agricultural and Forest Meteorology*, *218-219*, 11–24. https://doi.org/10.1016/j.agrformet.2015.11.010

Beckschäfer, P., Seidel, D., Kleinn, C., & Xu, J. (2013). On the exposure of hemispherical photographs in forests. *IForest - Biogeosciences & Forestry*, *6*(4), Article 957, 228–237. https://doi.org/10.3832/ifor0957-006

Bréda, N. J. J. (2003). Ground-based measurements of leaf area index: A review of methods, instruments and current controversies. *Journal of Experimental Botany*, *54*(392), 2403–2417. https://doi.org/10.1093/jxb/erg263

Brown, L. A., Meier, C., Morris, H., Pastor-Guzman, J., Bai, G., Lerebourg, C., Gobron, N., Lanconelli, C., Clerici, M., & Dash, J. (2020). Evaluation of global leaf area index and fraction of absorbed photosynthetically active radiation products over North America using copernicus ground based observations for validation data. *Remote Sensing of Environment*, *247*, 111935. https://doi.org/10.1016/j.rse.2020.111935

Brown, L. A., Morris, H., Meier, C., Knohl, A., Lanconelli, C., Gobron, N., Dash, J., & Danson, F. M. (2023). Stage 1 validation of plant area index from the global ecosystem dynamics investigation. *IEEE Geoscience & Remote Sensing Letters*, *20*, 1–5. https://doi.org/10.1109/LGRS.2023.3319528

Chen, J. M., & Black, T. A. (1992). Defining leaf area index for non-flat leaves. *Plant, Cell & Environment*, *15*(4), 421–429. https://doi.org/10.1111/j.1365-3040.1992.tb00992.x

Chen, X., Yin, G., Wei, S., Teo, H. C., Liu, G., & Tang, H. (2023). Intercomparison of multiple high-resolution LAI remote sensing products over neon forest sites. *IEEE International Geoscience and Remote Sensing Symposium 2023*, Pasadena, California, USA.

Djamai, N., Fernandes, R., Weiss, M., McNairn, H., & Goïta, K. (2019). Validation of the sentinel simplified level 2 product prototype processor (SL2P) for mapping cropland biophysical variables using sentinel-2/MSI and Landsat-8/OLI data. *Remote Sensing of Environment*, *225*, 416–430. https://doi.org/10.1016/j.rse.2019.03.020

Dorado-Roda, I., Pascual, A., Godinho, S., Silva, C., Botequim, B., Rodríguez-Gonzálvez, P., González-Ferreiro, E., & Guerra-Hernández, J. (2021). Assessing the accuracy of GEDI data for canopy height and aboveground biomass estimates in Mediterranean forests. *Remote Sensing*, *13*(12), 2279. https://doi.org/10.3390/rs13122279

Dubayah, R., & Blair, J. B. (2021a, April). *Global ecosystem dynamics investigation (GEDI) level 2 user guide: For SDPS PGEVersion 3 (P003) of GEDI L2A data and SDPS PGEVersion 3 (P003) of GEDI L2B data*. https://lpdaac.usgs.gov/documents/986/GEDI02_UserGuide_V2.pdf

Dubayah, R., Tang, H., Armston, J., Luthcke, S., Hofton, M., & Blair, J. (2021b). *GEDI L2B canopy cover and vertical profile metrics data global footprint level V002 [Data set]*. NASA EOSDIS Land Processes Distributed Active Archive Center. https://doi.org/10.5067/GEDI/GEDI02_B.002

Eriksson, H., & Eklundh, L. (2005). Variation of satellite estimated LAI due to the impact of the ground vegetation cover. *31st International Symposium on Remote Sensing of Environment, ISRSE 2005*. https://www.isprs.org/proceedings/2005/isrse/html/papers/648.pdf

Fang, H., Baret, F., Plummer, S., & Schaepman-Strub, G. (2019). An overview of global leaf area index (LAI): Methods, products, validation, and applications. *Reviews of Geophysics*, *57*(3), 739–799. https://doi.org/10.1029/2018RG000608

Fayad, I., Baghdadi, N., Alcarde Alvares, C., Stape, J. L., Bailly, J. S., Scolforo, H. F., Cegatta, I. R., Zribi, M., & Le Maire, G. (2021). Terrain slope effect on forest height and wood volume estimation from GEDI data. *Remote Sensing*, *13*(11), 2136. https://doi.org/10.3390/rs13112136

Fernandes, R., Plummer, S., Nightingale, J., Baret, F., Camacho, F., Fang, H., Garrigues, S., Gobron, N., Lang, M., Lacaze, R., Leblanc, S., Meroni, M., Martinez, B., Nilson, T., Pinty, B., Pisek, J., Sonnentag, O., Verger, A., Welles, J., & Widlowski, J. L. (2014, August). *Global leaf area index product validation good Practices. (Best practice for satellite-derived land product validation)*. Land Product Validation Subgroup (WGCV/CEOS). https://doi.org/10.5067/doc/ceoswgcv/lpv/lai.002

Filipponi, F. (2019). Exploitation of Sentinel-2 time series to map burned areas at the national level: A case study on the 2017 Italy wildfires. *Remote Sensing*, *11*(6), 622. https://doi.org/10.3390/rs11060622

Filipponi, F. (2021, May 3). *Comparison of LAI estimates from high resolution satellite observations using different biophysical processors*. Italian Institute for Environmental Protection and Research. 1st International Electronic Conference on Agronomy (IECAG). Available online: https://sciforum.net/event/iecag2021?section=#welcome.

Filipponi, F., Smiraglia, D., & Agrillo, E. (2022). Earth observation for phenological metrics (EO4PM): Temporal discriminant to characterize forest ecosystems. *Remote Sensing*, *14*(3), 721. https://doi.org/10.3390/rs14030721

Gao, Y., Skutsch, M., Paneque-Gálvez, J., & Ghilardi, A. (2020). Remote sensing of forest degradation: A review. *Environmental Research Letters*, *15*(10), 103001. https://doi.org/10.1088/1748-9326/abaad7

Global Climate Observing System. (2022). *The 2022 GCOS ECVs requirements*. World Meteorological Organization. https://library.wmo.int/viewer/58111/download?file=GCOS-245_2022_GCOS_ECVs_Requirements.pdf&type=pdf&navigator=1

Heiskanen, J., Rautiainen, M., Stenberg, P., Mõttus, M., & Vesanto, V. -H. (2013). Sensitivity of narrowband

vegetation indices to boreal forest LAI, reflectance seasonality and species composition. *Isprs Journal of Photogrammetry & Remote Sensing*, *78*, 1–14. https://doi.org/10.1016/j.isprsjprs.2013.01.001

Hijmans, R. J., Bivand, R., Pebesma, E., & Summer, M. D. (2023). *Terra: Spatial data analysis*. https://cran.r-project.org/web/packages/terra/terra.pdf

Hu, Q., Yang, J., Xu, B., Huang, J., Memon, M. S., Yin, G., Zeng, Y., Zhao, J., & Liu, K. (2020). Evaluation of global decametric-resolution LAI, FAPAR and FVC estimates derived from sentinel-2 imagery. *Remote Sensing*, *12*(6), 912. https://doi.org/10.3390/rs12060912

Hu, R., Yan, G., Nerry, F., Liu, Y., Jiang, Y., Wang, S., Chen, Y., Mu, X., Zhang, W., & Xie, D. (2018). Using airborne laser scanner and path length distribution model to quantify clumping effect and estimate leaf area index. *IEEE Transactions on Geoscience & Remote Sensing*, *56*(6), 3196–3209. https://doi.org/10.1109/TGRS.2018.2794504

Immitzer, M., Neuwirth, M., Böck, S., Brenner, H., Vuolo, F., & Atzberger, C. (2019). Optimal input features for tree species classification in central Europe based on multi-temporal sentinel-2 data. *Remote Sensing*, *11*(22), 2599. https://doi.org/10.3390/rs11222599

Kacic, P., Thonfeld, F., Gessner, U., & Kuenzer, C. (2023). Forest structure characterization in Germany: Novel products and analysis based on GEDI, sentinel-1 and sentinel-2 data. *Remote Sensing*, *15*(8), 1969. https://doi.org/10.3390/rs15081969

Kronenberg, R., Franke, J., Neumann, T., Struve, S., Bernhofer, C., & Sommer, W. (2021). Das Regionale Klimainformationssystem ReKIS – eine gemeinsame Plattform für Sachsen, Sachsen-Anhalt und Thüringen. In P. Fischer-Stabel (Ed.), *Umweltinformationssysteme: Grundlagen einer angewandten Geoinformatik/Geo-IT* (3rd ed. pp. 1–9). Wichmann. https://rekis.hydro.tu-dresden.de/wp-content/uploads/2022/03/ReKIS_Text_2021-01-22.pdf

Lacaze, R., Smets, B., Baret, F., Weiss, M., Ramon, D., Montersleet, B., Wandrebeck, L., Calvet, J. -C., Roujean, J. -L., & Camacho, F. (2015). Operational 333m biophysical products of the copernicus global land service for agriculture monitoring. *International Archives of the Photogrammetry, Remote Sensing and Spatial Information Sciences*, *XL-7*(W3), 53–56. https://doi.org/10.5194/isprsarchives-XL-7-W3-53-2015

Landesamt für Bodenmanagement und Geoinformation. (2019). *Digitales Geländemodell 5 m x 5 m*. Freistaat Thüringen. https://tlbg.thueringen.de/geobasisdaten/3d-informationen/digitale-gelaendemodelle

Lee, J., Cha, S., Lim, J., Chun, J., & Jang, K. (2023). Practical LAI estimation with DHP images in complex forest structure with rugged terrain. *Forests*, *14*(10), 2047. https://doi.org/10.3390/f14102047

Liang, S., & Wang, J. (2020). Fractional vegetation cover. In S. Liang & J. Wang (Eds.), *Advanced remote sensing* (2nd) (pp. 477–510). Academic Press. https://doi.org/10.1016/B978-0-12-815826-5.00012-X

LI-COR Biosciences. (2016). *LAI-2200 plant canopy analyzer instruction manual*. https://www.licor.com/env/support/MicroContent/Resources/MicroContent/manuals/lai-2200c-instruction-manuals.html

Liu, A., Cheng, X., & Chen, Z. (2021). Performance evaluation of GEDI and ICESat-2 laser altimeter data for terrain and canopy height retrievals. *Remote Sensing of Environment*, *264*, 112571. https://doi.org/10.1016/j.rse.2021.112571

Löw, M., & Koukal, T. (2020). Phenology modelling and forest disturbance mapping with Sentinel-2 time series in Austria. *Remote Sensing*, *12*(24), 4191. https://doi.org/10.3390/rs12244191

Majasalmi, T., Rautiainen, M., Stenberg, P., & Rita, H. (2012). Optimizing the sampling scheme for LAI-2000 measurements in a boreal forest. *Agricultural and Forest Meteorology*, *154-155*, 38–43. https://doi.org/10.1016/j.agrformet.2011.10.002

Marinelli, D., Dalponte, M., Frizzera, L., Næsset, E., & Gianelle, D. (2023). A method for continuous sub-annual mapping of forest disturbances using optical time series. *Remote Sensing of Environment*, *299*, 113852. https://doi.org/10.1016/j.rse.2023.113852

Markus, T., Neumann, T., Martino, A., Abdalati, W., Brunt, K., Csatho, B., Farrell, S., Fricker, H., Gardner, A., Harding, D., Jasinski, M., Kwok, R., Magruder, L., Lubin, D., Luthcke, S., Morison, J., Nelson, R., Neuenschwander, A., Palm, S., & Zwally, J. (2017). The ice, cloud, and land elevation satellite-2 (ICESat-2): Science requirements, concept, and implementation. *Remote Sensing of Environment*, *190*, 260–273. https://doi.org/10.1016/j.rse.2016.12.029

Marselis, S. M., Abernethy, K., Alonso, A., Armston, J., Baker, T. R., Bastin, J. -., Bogaert, J., Boyd, D. S., Boeckx, P., Burslem, D. F. R. P., Chazdon, R., Clark, D. B., Coomes, D., Duncanson, L., Hancock, S., Hill, R., Hopkinson, C., Kearsley, E., Kellner, J. R., & Dubayah, R. (2020). Evaluating the potential of full-waveform lidar for mapping pan-tropical tree species richness. *Global Ecology & Biogeography*, *29*(10), 1799–1816. https://doi.org/10.1111/geb.13158

Mougin, E., Demarez, V., Diawara, M., Hiernaux, P., Soumaguel, N., & Berg, A. (2014). Estimation of LAI, fAPAR and fCover of Sahel rangelands (Gourma, Mali). *Agricultural and Forest Meteorology*, *198-199*, 155–167. https://doi.org/10.1016/j.agrformet.2014.08.006

Münder, K., Seltmann, C. T., & Wernicke, J. (2022). Schlussbericht zum Verbundvorhaben: Bewirtschaftung der Fichte im Mittelgebirge unter Berücksichtigung des aktuellen Wachstumsgangs und Risikoabschätzung. https://doi.org/10.13140/RG.2.2.19056.12804

Mutanga, O., Masenyama, A., & Sibanda, M. (2023). Spectral saturation in the remote sensing of high-density vegetation traits: A systematic review of progress, challenges, and prospects. *Isprs Journal of Photogrammetry & Remote Sensing*, *198*, 297–309. https://doi.org/10.1016/j.isprsjprs.2023.03.010

Nagelkerke, N. J. D. (1991). A note on a general definition of the coefficient of determination. *Biometrika*, *78*(3), 691–692. https://doi.org/10.1093/biomet/78.3.691

Ni-Meister, W., Jupp, D. L. B., & Dubayah, R. (2001). Modeling lidar waveforms in heterogeneous and discrete canopies. *IEEE Transactions on Geoscience & Remote Sensing*, *39*(9), 1943–1958. https://doi.org/10.1109/36.951085

Ochtyra, A., Marcinkowska-Ochtyra, A., & Raczko, E. (2020). Threshold- and trend-based vegetation change monitoring algorithm based on the inter-annual multi-temporal normalized difference moisture index series: A case study of the tatra mountains. *Remote Sensing of Environment*, *249*, 112026. https://doi.org/10.1016/j.rse.2020.112026

Ogutu, B. O., Dash, J., & Dawson, T. P. (2013). Developing a diagnostic model for estimating terrestrial vegetation gross primary productivity using the photosynthetic quantum yield and Earth observation data. *Global Change Biology*, *19*(9), 2878–2892. https://doi.org/10.1111/gcb.12261

Patacca, M., Lindner, M., Lucas-Borja, M. E., Cordonnier, T., Fidej, G., Gardiner, B., Hauf, Y., Jasinevičius, G., Labonne, S., Linkevičius, E., Mahnken, M., Milanovic, S., Nabuurs, G. -J., Nagel, T. A., Nikinmaa, L., Panyatov, M., Bercak, R., Seidl, R., Ostrogović Sever, M. Z., & Schelhaas, M. -J. (2023). Significant increase in natural disturbance impacts on European forests since 1950. *Global Change Biology*, *29*(5), 1359–1376. https://doi.org/10.1111/gcb.16531

Persson, M., Lindberg, E., & Reese, H. (2018). Tree species classification with multi-temporal sentinel-2 data. *Remote Sensing*, *10*(11), 1794. https://doi.org/10.3390/rs10111794

Phiri, D., Simwanda, M., Salekin, S., Nyirenda, V., Murayama, Y., & Ranagalage, M. (2020). Sentinel-2 data for land cover/use mapping: A review. *Remote Sensing*, *12*(14), 2291. https://doi.org/10.3390/rs12142291

Potapov, P., Li, X., Hernandez-Serna, A., Tyukavina, A., Hansen, M. C., Kommareddy, A., Pickens, A., Turubanova, S., Tang, H., Silva, C. E., Armston, J., Dubayah, R., Blair, J. B., & Hofton, M. (2021). Mapping global forest canopy height through integration of GEDI and Landsat data. *Remote Sensing of Environment*, *253*, 112165. https://doi.org/10.1016/j.rse.2020.112165

Putzenlechner, B., Koal, P., Kappas, M., Löw, M., Mundhenk, P., Tischer, A., Wernicke, J., & Koukal, T. (2023). Towards precision forestry: Drought response from remote sensing-based disturbance monitoring and fine-scale soil information in Central Europe. *Science of the Total Environment*, *880*, 163114. https://doi.org/10.1016/j.scitotenv.2023.163114

Rautiainen, M., Lukeš, P., Homolová, L., Hovi, A., Pisek, J., & Mõttus, M. (2018). Spectral properties of coniferous forests: A review of in situ and laboratory measurements. *Remote Sensing*, *10*(2), 207. https://doi.org/10.3390/rs10020207

Richardson, A. D., Keenan, T. F., Migliavacca, M., Ryu, Y., Sonnentag, O., & Toomey, M. (2013). Climate change, phenology, and phenological control of vegetation feedbacks to the climate system. *Agricultural and Forest Meteorology*, *169*, 156–173. https://doi.org/10.1016/j.agrformet.2012.09.012

Richter, K., Atzberger, C., Hank, T. B., & Mauser, W. (2012a). Derivation of biophysical variables from Earth observation data: Validation and statistical measures. *Journal of Applied Remote Sensing*, *6*(1), 063557–1. https://doi.org/10.1117/1.JRS.6.063557

Richter, R., Louis, J., & Müller-Wilm, U. (2012b). *Sentinel-2 MSI-Level 2A products algorithm theoretical basis document*. https://forum.step.esa.int/uploads/default/original/2X/f/f3aa9be5ad9aab427885b536d0a30a5d47f45202.pdf

Scheffler, D., Hollstein, A., Diedrich, H., Segl, K., & Hostert, P. (2017). AROSICS: An automated and robust open-source image Co-registration software for multi-sensor satellite data. *Remote Sensing*, *9*(7), 676. https://doi.org/10.3390/rs9070676

Schneider, F. D., Ferraz, A., Hancock, S., Duncanson, L. I., Dubayah, R. O., Pavlick, R. P., & Schimel, D. S. (2020). Towards mapping the diversity of canopy structure from space with GEDI. *Environmental Research Letters*, *15*(11), 115006. https://doi.org/10.1088/1748-9326/ab9e99

Sellers, P. J., Dickinson, R. E., Randall, D. A., Betts, A. K., Hall, F. G., Berry, J. A., Collatz, G. J., Denning, A. S., Mooney, H. A., Nobre, C. A., Sato, N., Field, C. B., & Henderson-Sellers, A. (1997). Modeling the exchanges of energy, water, and carbon between continents and the atmosphere. *Science*, *275*(5299), 502. https://doi.org/10.1126/science.275.5299.502

Senf, C., Buras, A., Zang, C. S., Rammig, A., & Seidl, R. (2020). Excess forest mortality is consistently linked to drought across Europe. *Nature Communications*, *11*(1), 6200. https://doi.org/10.1038/s41467-020-19924-1

Silva, C., Hamamura, C., Valbuena, R., Hancock, S., Cardil, A., Broadbent, E. N., Almeida, D., Silva Junior, C., & Klauberg, C. (2020). *rGEDI: NASA's global ecosystem dynamics investigation (GEDI) data visualization and processing. Version 0.1.9*. https://CRAN.R-project.org/package=rGEDI

Stritih, A., Seidl, R., & Senf, C. (2023). Alternative states in the structure of mountain forests across the Alps and the role of disturbance and recovery. *Landscape Ecology*, *38*(4), 933–947. https://doi.org/10.1007/s10980-023-01597-y

Tang, H., & Armston, J. (2019, December, 6). *Algorithm theoretical basis document (ATBD) for GEDI L2B footprint canopy cover and vertical profile metrics: Version 1.0*. University of Maryland. https://lpdaac.usgs.gov/documents/588/GEDI_FCCVPM_ATBD_v1.0.pdf

Thonfeld, F., Gessner, U., Holzwarth, S., Kriese, J., Da Ponte, E., Huth, J., & Kuenzer, C. (2022). A first assessment of canopy cover loss in Germany's forests after the 2018–2020 drought years. *Remote Sensing*, *14*(3), 562. https://doi.org/10.3390/rs14030562

ThüringenForst. (2022). *Digitale forstliche Standortskarte Thüringen*.

TLUBN. (2006). *Bodengeologische Karte von Thüringen/Soil geological map of Thuringia*. Weimar. https://geomis.geoportal-th.de/geonetwork/srv/api/records/613EC54D-F759-4F0F-A00B-55A307F43015

Törnros, T., & Menzel, L. (2014). Leaf area index as a function of precipitation within a hydrological model. *Hydrology Research*, *45*(4–5), 660–672. https://doi.org/10.2166/nh.2013.143

Verrelst, J., Camps-Valls, G., Muñoz-Marí, J., Rivera, J. P., Veroustraete, F., Clevers, J. G., & Moreno, J. (2015). Optical remote sensing and the retrieval of terrestrial vegetation bio-geophysical properties – a review. *Isprs Journal of Photogrammetry & Remote Sensing*, *108*, 273–290. https://doi.org/10.1016/j.isprsjprs.2015.05.005

Wang, C., Jia, D., Lei, S., Numata, I., & Tian, L. (2023a). Accuracy assessment and impact factor analysis of GEDI leaf area index product in temperate forest. *Remote Sensing*, *15*(6), 1535. https://doi.org/10.3390/rs15061535

Wang, Y., Fang, H., Zhang, Y., Li, S., Pang, Y., Ma, T., & Li, Y. (2023b). Retrieval and validation of vertical LAI profile derived from airborne and spaceborne LiDAR data at a deciduous needleleaf forest site. *GIScience & Remote Sensing*, *60*(1), Article 2214987. https://doi.org/10.1080/15481603.2023.2214987

Weiss, M., & Baret, F. (2017, October, 10). *CAN EYE V6.4.91 user manual*. INRA.

Weiss, M., Baret, F., & Jay, S. (2020). *S2toolbox level 2 products. Version 2.0*. http://step.esa.int/docs/extra/ATBD_S2ToolBox_V2.0.pdf

Wernicke, J., Seltmann, C. T., Wenzel, R., Becker, C., & Körner, M. (2022). Forest canopy stratification based on fused, imbalanced and collinear LiDAR and sentinel-2 metrics. *Remote Sensing of Environment*, *279*, 113134. https://doi.org/10.1016/j.rse.2022.113134

Xiao, J., Chevallier, F., Gomez, C., Guanter, L., Hicke, J. A., Huete, A. R., Ichii, K., Ni, W., Pang, Y., Rahman, A. F., Sun, G., Yuan, W.,

Zhang, L., & Zhang, X. (2019). Remote sensing of the terrestrial carbon cycle: A review of advances over 50 years. *Remote Sensing of Environment*, *233*, 111383. https://doi.org/10.1016/j.rse.2019.111383

Yan, K., Park, T., Chen, C., Xu, B., Song, W., Yang, B., Zeng, Y., Liu, Z., Yan, G., Knyazikhin, Y., & Myneni, R. B. (2018). Generating global products of LAI and FPAR from SNPP-VIIRS data: Theoretical background and implementation. *IEEE Transactions on Geoscience & Remote Sensing*, *56*(4), 2119–2137. https://doi.org/10.1109/TGRS.2017.2775247

Yan, K., Park, T., Yan, G., Chen, C., Yang, B., Liu, Z., Nemani, R., Knyazikhin, Y., & Myneni, R. (2016). Evaluation of MODIS LAI/FPAR product collection 6. Part 1: Consistency and improvements. *Remote Sensing*, *8* (5), 359. https://doi.org/10.3390/rs8050359

Zhang, J., Tian, J., Li, X., Wang, L., Chen, B., Gong, H., Ni, R., Zhou, B., & Yang, C. (2021). Leaf area index retrieval with ICESat-2 photon counting LiDAR. *International Journal of Applied Earth Observation and Geoinformation*, *103*, 102488. https://doi.org/10.1016/j.jag.2021.102488

Appendix

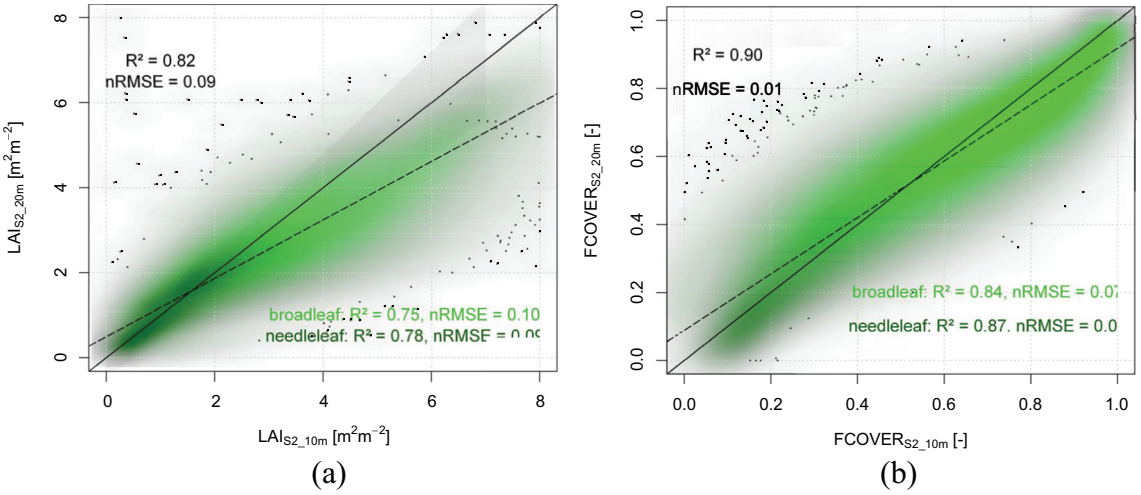

Figure A1. Sentinel-2 derived biophysical products (a) LAI and (b) FCOVER, with the products obtained from the 10 m version of the algorithm plotted against the products from the 20 m version (within the "biophysical Processor" in SNAP), respectively. The continuous line represents the 1:1 line, the grey-coloured polygon refers to the 90% confidence intervals for the linear regression model shown as dashed line. For LAI (a), the second grey-coloured polygon around the 1:1 line refers to the GCOS uncertainty requirement.

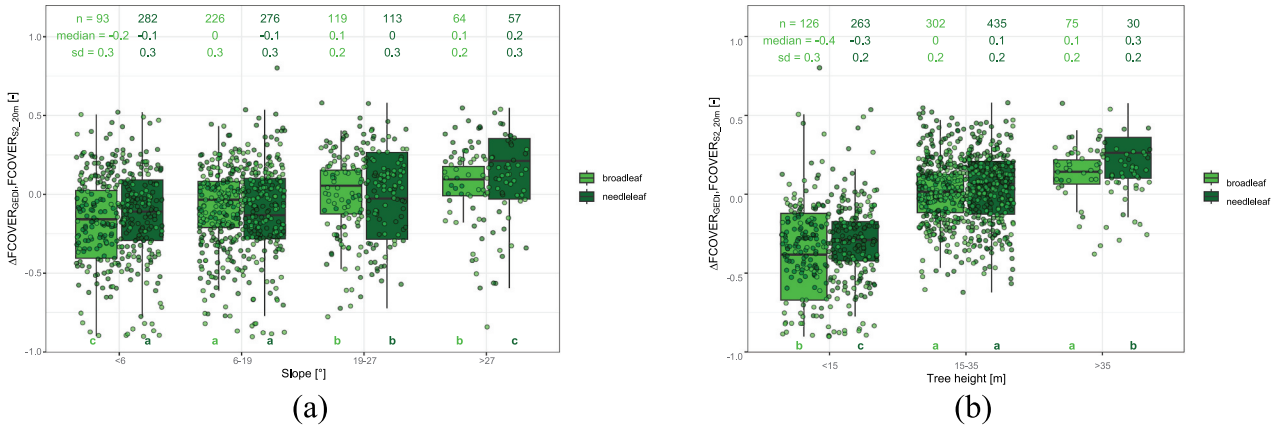

Figure A2. Deviation between GEDI-derived FCOVER and Sentinel-2-derived FCOVER with respect to (a) terrain slope and (b) canopy height for needleleaf and broadleaf forest in the study area in summer 2021 and 2022. Different lowercase letters indicate significant ($p < 0.05$) differences with levels of terrain slope for PAI deviations.

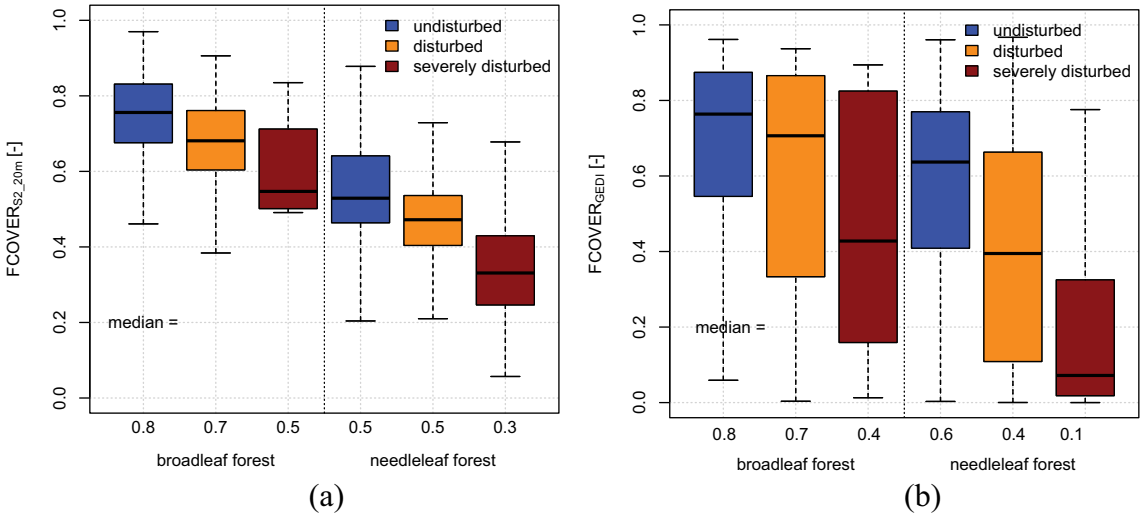

Figure A3. Sentinel-2-derived FCOVER (a) and GEDI-derived FCOVER (b) with regards to forest disturbance level and forest type.